The kinetic basis of threshold effects observed in mitochondrial diseases: a systemic approach

Thierry LETELLIER,* Reinhart HEINRICH,† Monique MALGAT* and Jean-Pierre MAZAT*‡

* Université Bordeaux II, 146 rue Léo-Saignat, F-33076 Bordeaux Cedex, France,
and † Fachbereich Biologie, Institut für Biophysik, Humboldt Universität zu Berlin, Invalidenstrasse, 42, D-10115, Berlin, Germany

Threshold effects in the expression of metabolic diseases have often been observed in mitochondrial pathologies, i.e. the clinical demonstration of the disease appears only when the activity of a step has been reduced to a rather low level. We show experimentally that an inhibition of cytochrome *c* oxidase activity by cyanide, simulating a defect in this step, leads to a decrease in mitochondrial respiration which then exhibits a threshold behaviour similar to that observed in mitochondrial diseases. We discuss this behaviour in terms of metabolic control theory and construct a mathematical model simulating this behaviour.

INTRODUCTION

Threshold effects have recently been described in mitochondrial diseases, particularly by Wallace and co-workers [1,2] who showed them to be related to the balance between normal and mutant mitochondrial (mt) DNA (mt DNA heteroplasmy). We think that a crucial stage in the expression of a threshold in clinical diseases may be due to the action of a localized defect in a given step on the global flux of a metabolic pathway. Thus it was observed by Bindoff [3], both in a patient with cytochrome *c* oxidase deficiency and in an animal model (copper-deficient rat), that lowering the activity of complex-IV by over 50% did not affect the respiratory flux.

We have considered this problem from an experimental point of view by progressively inhibiting the activity of cytochrome *c* oxidase of mitochondria isolated from rat muscle with increasing concentrations of KCN, thus mimicking the effect of various degrees of a defect in the activity of this enzyme.

MATERIALS AND METHODS

Rat muscle mitochondria were isolated by differential centrifugations as described by Morgan-Hughes et al. [4]. Protein concentration was estimated by the biuret method using BSA as a standard. Mitochondrial oxygen consumption was monitored at 30 °C in a 1 ml thermostatically controlled closed vessel with rapid stirring and equipped with a Clark oxygen electrode, in the following buffer: 75 mM mannitol, 25 mM sucrose, 100 mM KCl, 10 mM Tris phosphate, 10 mM Tris/HCl, pH 7.4, 50 μM EDTA, with 10 mM pyruvate and 10 mM malate as respiratory substrates to record the respiration rate of the whole chain, or in the presence of 0.50 mM ascorbate and 0.25 mM *NNN'N'*-tetramethyl-*p*-phenylenediamine (TMPD) and 10 μg/ml antimycin to record the activity of cytochrome *c* oxidase alone. The mitochondrial concentration used in this study was 1 mg/ml and state 3 (according to Chance and Williams [5]) was obtained by addition of 1.2 mM ADP. We also measured cytochrome *c* oxidase activity spectrophotometrically following oxidation of cytochrome *c* at 550 nm [6].

Non-linear curve fitting was done using the program 'Simfit' [7] and simulations with the program TK Solver Plus (Universal Technical Systems, Rockford, IL, U.S.A.).

RESULTS

In parallel cyanide titration experiments, it is possible to record the remaining cytochrome *c* oxidase activity and the resulting respiration rate. Figure 1 shows a typical experiment where both curves correspond to experiments performed on three batches of mitochondrial preparations. The fact that the direct spectrophotometrical titration of cytochrome *c* oxidase with cyanide gave the same inhibition curve as the titration of oxygen consumption, with ascorbate and TMPD as substrate, indicates that in the latter case, due to high TMPD concentration, the cytochrome *c* oxidase activity is the 'rate-limiting step', or in other words it has a flux control coefficient of unity in this assay. The interest of recording the cytochrome *c* oxidase activity with ascorbate and TMPD is that this complex is in a similar environment to that used in recording the whole respiratory chain flux. It is of interest to note the shape of these curves. The inhibition curve of cytochrome *c* oxidase activity is quasi-linear for non-saturating inhibitory concentration with an inhibition nearly proportional to the KCN concentration added, while the variation in the respiratory rate as a function of KCN concentration is sigmoidal. The difference in these shapes is the basis of the threshold effect. For instance, a 50% inhibition of cytochrome *c* oxidase gives only 10% inhibition of the whole respiratory flux. Even 75% inhibition of the enzyme leads to only 20% inhibition of the flux. However, when the inhibition of cytochrome *c* oxidase activity increases beyond this value, the respiratory flux decreases sharply, giving rise to a threshold effect. This phenomenon is well illustrated in Figure 2, which gives the respiratory rate and cytochrome *c* oxidase activity of Figure 1 for the same values of inhibitory concentrations. These results are in accordance with the Bindoff observations [3] in a patient with cytochrome *c* oxidase deficiency, in the animal model of copper-deficient rats, and those of Hayashi et al. [8] and Chomyn et al. [9] on patient cybrids in culture.

These results are entirely consistent with metabolic control theory [10,11]. According to this theory, a control coefficient measures the effect of a small disturbance of a given step on a global flux in a metabolic network under steady-state conditions. This parameter can be evaluated in the present experiment by the ratio of the initial slope of the V_{O_2} inhibition curve (the observed

Abbreviations used: TMPD, *NNN'N'*-tetramethyl-*p*-phenylenediamine; mt, mitochondrial.

‡ To whom correspondence should be addressed.

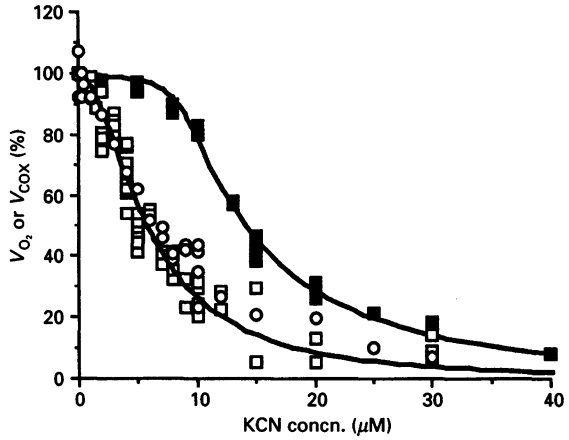

Figure 1. KCN inhibition of respiratory rate (■) and of cytochrome *c* oxidase activity [(□) using ascorbate/TMPD as substrates or (○) recording oxidation of reduced cytochrome *c* at 550 nm]

The points shown are from three different experiments carried out with three different mitochondrial preparations. The solid lines are theoretical fitted curves according to eqn. (5) and eqn. (6) respectively. The obtained values of the parameters in the fitting procedure are (in arbitrary units): $K_1^+ = 1$, $K_1^- = 2.24$, $K_2^+ = 1$; $V_1^+ = 0.33$, $V_1^- = 10^{-5}$, $V_2^+ = 1$, $n = 1.83$, $K_I = 5.67$, $S = 22$.

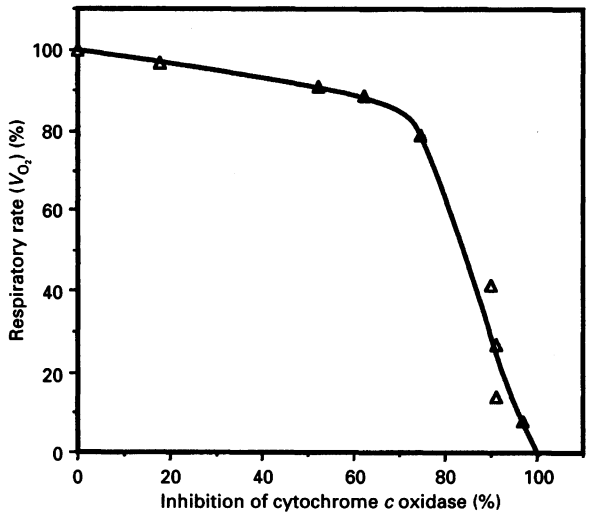

Figure 2. Respiratory rate as a function of cytochrome *c* oxidase inhibition

The points are the means of the data in Figure 1 corresponding to the same KCN concentrations.

disturbance of the flux) to the initial slope of the inhibition curve of the cytochrome *c* oxidase activity (the step disturbance). In our case, we find a control coefficient of the cytochrome *c* oxidase step of 0.12 on the mitochondrial respiration flux (V_{O_2}). Control theory has it that there are strong constraints on the control coefficients (e.g. sum equal to one) so the values of the control coefficients of the individual steps are usually low, which is the case in oxidative phosphorylation [12–15]. Thus the initial slope of the pathway flux inhibition curve is usually much gentler than the corresponding slope of the step inhibition curve; this is the case in Figure 1. However, both curves must come together at high inhibitory concentrations, when the cytochrome *c* oxidase

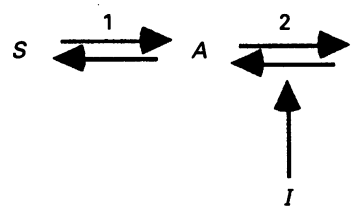

Scheme 1. Scheme of the reactions involved in the example

activity becomes very low. For higher inhibitory concentrations, however, the relationship between the steady-state flux and the remaining activity of the isolated step shown in Figure 1 can no longer be discussed in terms of control analysis, since, as regards the whole flux, changes in the metabolite concentrations occur. This is not the case in the inhibition curve of the isolated step.

To understand the threshold behaviour in Figure 2 better, we have used the model in Scheme 1. Step 2 could represent the cytochrome *c* oxidase complex, step 1 summarizes the preceding reactions of the respiratory chain; *S*, the respiratory substrate, and *A*, the reduced cytochrome *c*. We assume furthermore that step 2 is practically irreversible. In this case, the model is completely described by the kinetic equations of reactions 1 and 2. For simplicity, we assume Michaelis–Menten equations for these rate functions:

$$v_1 = \frac{V_1^+ \frac{S}{K_1^+} - V_1^- \frac{A}{K_1^-}}{1 + \frac{S}{K_1^+} + \frac{A}{K_1^-}} \tag{1}$$

and

$$v_2 = \frac{V_2^+}{1 + \left(\frac{I}{K_I}\right)^n} \cdot \frac{\frac{A}{K_2^+}}{1 + \frac{A}{K_2^+}} \tag{2}$$

V_1^+ and V_1^- are the maximal activities of the forward and the backward reactions of step 1. V_2^+ is the forward maximal rate of reaction 2, which is supposed to be irreversible. K_1^+ is the Michaelis constant of *S* for enzyme 1; K_1^- is the Michaelis constant of *A* for enzyme 1, and K_2^+ is the Michaelis constant of *A* for enzyme 2.

The inhibition of step 2 is assumed to be non-competitive, with K_I as the inhibitory constant, thus affecting only the maximal activity V_2^+ of reaction 2 (in a co-operative manner).

This model is given to show that a threshold effect could be commonly observed in metabolic networks. It does not intend to present exact modelling of the respiratory chain or of the cytochrome *c* oxidase kinetics.

From the steady-state condition $v_1 = v_2$, we can derive the steady-state concentration A^* by solving a quadratic equation for different values of *I*. The value of A^* for $I = 0$ will be denoted A_0^*. The activity of the isolated step as a function of *I* is defined by:

$$v_2(I) = v_2(A_0^*, I) \tag{3}$$

while the steady-state flux $J(I)$ is given by the equation:

$$J(I) = v_2[A^*(I), I] \tag{4}$$

For comparison of the curves given by eqns. (3) and (4), it is

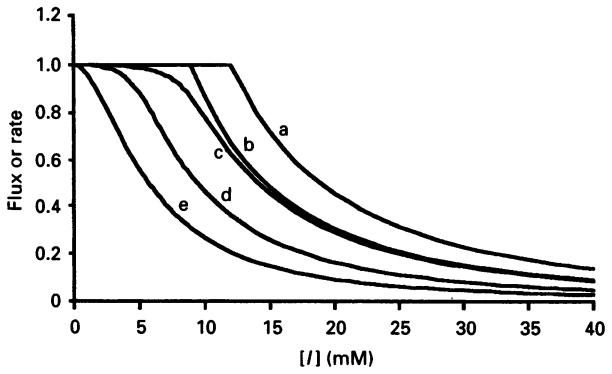

Figure 3. Simulated inhibition curves

The following values of the parameters were used: $K_1^+ = 1$, $K_1^- = 2.24$, $K_2^+ = 1$; $V_1^- = 10^{-5}$, $V_2^+ = 1$, $n = 1.83$, $K_I = 5.67$, and: (**a**) $V_1^+ = 0.2$ and $S = 10000$; (**b**) $V_1^+ = 0.3$ and $S = 10000$; (**c**) $V_1^+ = 0.33$ and $S = 22$ (corresponding to Figure 1); (**d**) $V_1^+ = 0.6$ and $S = 22$; (**e**) $= v_2^{norm}$ (eqn. 5).

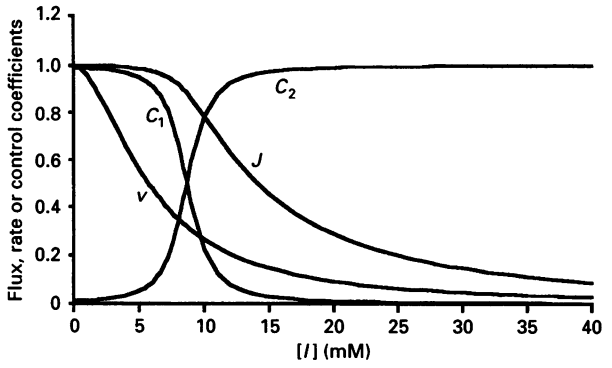

Figure 4. Variation in the control coefficients of the flux by step 1 (C_1^J) and by step 2 (C_2^J) as a function of inhibitor concentration [*I*] for the values of the parameters listed in the legend to Figure 1

useful to normalize them by the value of the flux at $I = 0$. We obtain:

$$v_2^{norm}(I) = \frac{1}{1+\left(\frac{I}{K_I}\right)^n} \tag{5}$$

and

$$J^{norm}(I) = \frac{A^*(I)}{A_0^*} \cdot \frac{1+\frac{A_0^*}{K_2^+}}{1+\frac{A^*(I)}{K_2^+}} \cdot \frac{1}{1+\left(\frac{I}{K_I}\right)^n} \tag{6}$$

The solid lines in Figure 1 are obtained by fitting the experimental points to the rate equations (5) and (6). The parametric values obtained are listed in the legend of Figure 1.

Figure 3 shows some simulated curves for different values of the parameters S and V_1^+, clearly demonstrating the possible existence of a threshold. This effect is more pronounced at higher concentrations of the initial substrate S. In the limiting case of a saturating concentration of S, the curve $J^{norm}(I)$ first shows a plateau then, beyond a critical inhibitory concentration ($I_{crit.}$), the inhibition of the steady-state flux parallels that of the isolated step.

The plateau shown in Figure 3 may be explained as follows. An inhibition of the second step will affect the steady-state flux through inhibition of the first step by increasing the concentration of A. When S is very high, A also has to become rather high to have an effect. This can only occur if the apparent maximal rate of the second step $V_2^+/[1+(I/K_I)^n]$ is less than or equal to the maximal rate V_1^+ of the forward reaction of step 1, so that for $S \gg K_1^+$, $I_{crit.}$ is given by:

$$\frac{V_2^+}{1+\left(\frac{I_{crit.}}{K_I}\right)^n} = V_1^+ \quad \text{or} \quad \left(\frac{I_{crit.}}{K_I}\right)^n = \frac{V_2^+}{V_1^+} - 1 \tag{7}$$

Beyond that point, A is saturating for the second reaction; what is then observed is just the non-competitive inhibition of this step.

Each steady state for a given inhibitory concentration may be characterized by its own flux control coefficients which can be calculated from the equations:

$$C_1^J = \frac{\epsilon_A^2}{\epsilon_A^2 - \epsilon_A^1} \quad \text{and} \quad C_2^J = -\frac{\epsilon_A^1}{\epsilon_A^2 - \epsilon_A^1} \tag{8a,b}$$

which follow immediately from the summation and the connectivity theorem of control analysis [16].

The elasticities are defined by:

$$\epsilon_A^1 = \frac{\partial v_1}{\partial A} \quad \text{and} \quad \epsilon_A^2 = \frac{\partial v_2}{\partial A} \tag{9a,b}$$

so that ϵ_A^1 and ϵ_A^2 can be easily calculated from the rate equations [1,2], taking into account the value of $A^*(I)$. Due to the fact that logarithmic and unscaled flux control coefficients are equal for a linear pathway [17] we have used unscaled elasticities (eqns. 9a,b). The variations in the control coefficients C_1^J and C_2^J as a function of I are shown in Figure 4 for the same values of S as in Figure 1. With increasing inhibitory concentrations, there is a transition of the control coefficient C_2^J from a very low value to a value almost equal to one. At very high concentrations of S, this transition is very sharp and occurs at the critical value of $I(I_{crit.})$ already encountered in Figure 3. This shows that a threshold of the type described in Figure 1 is accompanied by a drastic change from a low to a high control coefficient of the inhibited step, in a narrow range of inhibitory concentrations. This situation is equivalent to that encountered with different patients exhibiting various levels of a defect in a given step of the oxidative-phosphorylation pathway.

DISCUSSION

Threshold effects are often observed in mitochondrial diseases [1,2]. We have experimentally stimulated such an effect by decreasing the activity of cytochrome *c* oxidase in isolated muscle mitochondria using increased concentrations of the specific inhibitor cyanide, thus mimicking various degrees of a defect in this complex.

Our results show a very clear threshold in respiration, which remains nearly maximal until a low level of cytochrome *c* oxidase activity is reached. At this level, an abrupt decrease in the respiratory rate is observed (Figures 1 and 2). We have built a

very simple example (Scheme 1) to explain the fundamental basis leading to a threshold effect. The behaviour is related to a low control coefficient of the step on the flux under study and is inescapable in this case. Such an effect has also been observed in the case of complex III on the oxidative flux or on succinate cytochrome *c* oxidase flux in rat muscle mitochondria [18,19].

How can this direct threshold effect be related to the heteroplasmy of mtDNA, which may be observed in mitochondrial diseases [8,9]? First, it might be thought that the activity decrease of a given step (e.g. cytochrome *c* oxidase) is proportional to the percentage of mutant mtDNA, in which case the profile of Figure 2 would remain unchanged when plotting the percentage of respiration rate as a function of the percentage of DNA heteroplasmy. A threshold effect in a flux due to DNA heteroplasmy has already been observed by Flint et al. [20,21]. They studied the rate of arginine production in heterokaryons of *Neurospora crassa* with different proportions of a mutant gene of the arginine pathway. This phenomenon was extensively discussed by Kacser and Burns [22]. A more precise quantification of the heteroplasmy effect on the activity level of a given step would require measurement on the one hand of its influence on the amount of transcribed normal mtDNA and on the other hand of translated normal transcripts. At these particular stages, a threshold effect could also occur [8,9]. Another question is to know the effects of defective mitochondria on the cellular metabolism as a whole. If mitochondrial metabolism is considered as a single step in the whole cellular metabolism, it may be hypothesized that a threshold effect can again occur which is analogous to that observed at the level of the whole mitochondrial metabolism. Thus there might be at least three levels at which threshold effects occur. The first is the expression of the heteroplasmy of DNA at the level of a given enzymic step; the second is the threshold effect observed in the mitochondrial metabolism as a result of a decrease in a given mitochondrial activity, which is the subject of this paper. The third may occur in the expression of defective mitochondria in the whole cellular metabolism. At each level the threshold effect will reinforce the others. Thus when the global effect of mtDNA heteroplasmy on the whole cellular metabolism and its clinical expression is considered, a very sharp threshold could be anticipated.

Received 16 November 1993/2 March 1994; accepted 8 March 1994

We are grateful to Professor J. Clark and to Dr. B. Groen and Joseph Clark for critically reading this manuscript, to Dr. R. Schuster and Dr. H. G. Holzhütter for the fitting of the experimental data and to R. Cook for correcting the English. This work was supported by the Association Française contre les Myopathies (A.F.M.), by the Region Aquitaine, by the University of Bordeaux II, and by the French–German PROCOPE Programme.

REFERENCES

1 Wallace, D. C. (1986) Somatic Cell Mol. Genet. **12**, 41–49
2 Shoffner, J. M., Lott, M. T., Lezza, A. M. S., Seibel, P., Ballinger, S. W. and Wallace, D. C. (1990) Cell **61**, 931–937
3 Bindoff, L. A. (1990) PhD thesis, Newcastle upon Tyne University
4 Morgan-Hughes, J. A., Hayes, D. J., Clark, J. B., Landon, D. N., Swash, M., Strak, R. J. and Rudge, P. (1982) Brain **105**, 553–582
5 Chance, B. and Williams, G. R. (1956) Adv. Enzymol. (Alberty, R. A., ed.) **17**, 65–134
6 Wharton, D. C. and Tzagoloff, A. (1967) Methods Enzymol. **10**, 245–250
7 Holzhütter, H. G. and Colosimo, A. (1990) Comput. Appl. Biosci. **6**, 23–28
8 Hayashi, J.-I., Ohta, S., Kikuchi, A., Takemitsu, M., Goto, Y.-I. and Nonaka, I. (1991) Proc. Natl. Acad. Sci. U.S.A. **88**, 10614–10618
9 Chomyn, A., Martinuzzi, A., Yoneda, M., Daga, A., Hurko, O., Johns, D., Lai, S. T., Nonaka, I., Angelini, C. and Attardi, G. (1992) Proc. Natl. Acad. Sci. U.S.A. **89**, 4221–4225
10 Kacser, H. and Burns, J. A. (1973) in Rate Control of Biological Processes (Davies, D. D., ed.), pp. 65–104, Cambridge University Press, Cambridge, U.K.
11 Heinrich, R. and Rapoport, T. A. (1974) Eur. J. Biochem. **42**, 89–95
12 Groen, A. K., Wanders, R. J. A., Westerhoff, H. V., Van Der Meer, R. and Tager, J. M. (1982) J. Biol. Chem. **257**, 2754–2757
13 Tager, J. M., Wanders, R. J. A., Groen, A. K., Kunz, W., Bohnensak, R., Kuster, U., Letko, G., Boehme, G., Duszynski, J. and Wojtczak, L. (1983) FEBS Lett. **151**, 1–9
14 Mazat, J.-P., Jean-Bart, E., Rigoulet, M. and Guerin, B. (1986) Biochim. Biophys. Acta **849**, 7–15
15 Letellier, T., Malgat, M. and Mazat, J.-P. (1993) Biochim. Biophys. Acta **1141**, 58–64
16 Mazat, J.-P., Reder, C. and Letellier, T. (1990) in Control of Metabolic Processes (Cornish-Bowden, A. and Cardenas, M. L., eds.). NATO ASI Series, vol. 190, pp. 129–138, Plenum Press, New York, and London
17 Reder, C. (1988) J. Theor. Biol. **135**, 175–201
18 Taylor, R. W., Birch-Machin, M. A., Bartlett, K. and Turnbull, M. (1993) Biochim. Biophys. Acta **1181**, 261–265
19 Taylor, R. W., Birch-Machin, M. A., Barlett, K., West, I. C. and Turnbull, M. (1994) J. Biol. Chem. **269**, 3523–3528
20 Flint, H. J., Porteous, D. J. and Kacser, H. (1980) Biochem. J. **190**, 1–15
21 Flint, H. J., Tateson, R. W., Barthelmess, I. B., Porteous, D. J., Donachie, W. D. and Kacser, H. (1981) Biochem. J. **200**, 231–246
22 Kacser, H. and Burns, J. A. (1981) Genetics **97**, 639–666